

UDK 669.717:661.96

## STUDIES OF HYDROLYSIS OF ALUMINUM ACTIVATED BY ADDITIONS OF Ga–In–Sn EUTECTIC ALLOY, BISMUTH OR ANTIMONY

F. D. MANILEVICH<sup>1</sup>, Yu. K. PIRSKYY<sup>1</sup>, B. I. DANIL'TSEV<sup>1</sup>,  
A. V. KUTSYI<sup>1</sup>, V. A. YARTYS<sup>2</sup>

<sup>1</sup> V. I. Vernadskii Institute of General and Inorganic Chemistry of the NASU;

<sup>2</sup> Institute for Energy Technology, Norway

The Ga–In–Sn eutectic-catalyzed interaction of aluminum alloys with water resulting in hydrolysis process and generation of hydrogen is studied. The aluminum alloys were prepared by melting aluminum with additions of Ga–In–Sn eutectic (5 wt.%), bismuth (3 wt.%) or antimony (3 wt.%). The temperature-dependent kinetics of their hydrolysis in a temperature range 25...70°C is studied by using a volumetric technique. The most efficient activation of the hydrolysis process is achieved for the Al–Ga–In–Sn alloy. Addition of bismuth to the Al–Ga–In–Sn alloy significantly reduces the hydrolysis rate, whereas the addition of antimony has only a slight effect on the process, even though the standard electrode potentials of bismuth and antimony show close values. The interactions of the studied alloys with water can be well fitted as a topochemical process. The modified Prout–Tompkins equation is employed to yield the effective hydrolysis rate constants, and it is found that they increase following the temperature rise in the temperature range from 25 to 70°C. The activation energies of the hydrolysis process for the studied alloys are calculated from the temperature dependence of the values of the effective rate constants, which indicate that in the main range of hydrogen generation (after the completion of the induction period and before the beginning of hydrogen release deceleration) the hydrolysis process can be described as a diffusion-limited one.

**Keywords:** *hydrolysis, aluminum alloys, hydrogen generation, Ga–In–Sn eutectic alloy, hydrolysis kinetics.*

**Introduction.** Hydrogen is an eco-friendly energy carrier with high energy content (122 MJ/kg) as well as a chemical, which has valuable reducing properties and is broadly used in chemical industry [1–3]. For the past decades hydrogen-based power generation, which employs hydrogen as an energy carrier and as a fuel, witnessed a significant development [1–5]. Particularly, the demand for fuel cells used for various purposes, in which hydrogen fuel is converted into electric current using anodic oxidation of hydrogen and corresponding cathodic process, has greatly increased. The development of autonomous power sources on the basis of fuel cells and hydrogen generators or H stores solves the problem of powering a wide range of portable electrical and electronic devices [1–7].

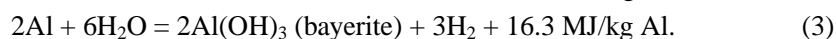
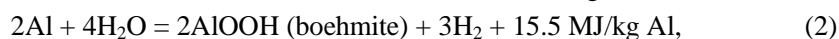
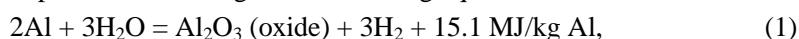
Expansion of application scopes and increase of the scale of used hydrogen calls for improving technologies for its production, transportation and storage. At present, the major part of hydrogen (80...90%) is produced from hydrocarbons, though their natural resources are running short [1, 8]. On the other hand, the Earth's hydrosphere contains around  $1.4 \cdot 10^{18}$  tonnes of water, H<sub>2</sub>O, providing unlimited resources of hydrogen. The electrochemical decomposition of liquid water or water vapor is a well-developed and long-used method of hydrogen production [1, 9, 10]. However, the electro-

chemical production of hydrogen from water needs a significant amount of electrical energy to split water molecules. Numerous investigations aimed at improving and optimizing the water electrolysis have not resulted in the reduction of hydrogen cost [1, 3, 5–7, 9, 10]. Methods of water splitting based on thermochemical cycles using the thermal energy (~800°C) of nuclear reactors or solar power plants are also applied [1, 11, 12]. The implementation of these methods requires complex engineering solutions and materials with high corrosion resistance. Photoelectrochemical water splitting using semiconductor materials is being developed as well [13–16]. Biochemical water splitting using specially derived types of algae and microorganisms has also been proposed [17, 18]. However, these methods have not found a wide practical use at present mainly because of their low efficiency and insufficient productivity.

Hydrogen generation using water by utilising various energy-storing substances (ESSs) and variable conditions are of considerable interest [19]. These conditions include chemical interaction between ESSs and water – hydrolysis reaction. Hydrogen generation from water using ESSs is carried out in hydrolysis-type hydrogen generators [20]. Such generators can be autonomous, portable and are convenient for the generation of hydrogen directly on site. Their use gives great benefits as this eliminates significant problems associated with the accumulation, storage and transportation of hydrogen.

To produce hydrogen by hydrolysis, binary and complex metal hydrides (MgH<sub>2</sub>, NaBH<sub>4</sub>, LiBH<sub>4</sub>, etc.), individual metals that can react with water (Al, Mg and other low-melting point metals) and their alloys, can be used [1, 19]. The hydrolysis of metal hydrides is accompanied by evolution of a much larger amount of hydrogen than the hydrolysis of metals, but hydrides are much more expensive than metals. Besides, they are hygroscopic, susceptible to atmospheric oxygen and require storage in a dry inert gas [21].

The aluminum-based ESSs are promising for the release of hydrogen from water. The advantages of aluminum in its use as ESS are its high energy capacity (31.1 MJ/kg) [2, 22], relatively low price (~1.8 USD/kg), high availability, low density, convenient and safe transportation and storage, fairly large productivity in terms of the amount of hydrogen that is evolved during its hydrolysis, and simplicity of hydrogen generation system. Depending on the conditions, three paths of the reaction of aluminum with water are possible according to the following equations:



All three reactions are exothermic and in all cases the amount of hydrogen evolved from water is the same and equals to 1244 L/kg of Al or 111 g/kg of Al [23–25]. The aluminum products obtained in a hydrolysis process are inert and eco-friendly substances which can be used to recuperate aluminum or to manufacture ceramics, absorbents, paper, fillers, etc. [1, 26–28].

Aluminum has a very negative value of standard electrode potential ( $E_{\text{Al}^{3+}/\text{Al}}^0 = -1.662 \text{ V}$ ) [29] and thus it reacts with water readily and rapidly in the absence of a protective film. However, under normal conditions the reaction of aluminum with water does not proceed since the aluminum surface is covered by a thin oxide film. To activate aluminum, this dense film must be removed or cracked to expose a bare surface of Al metal.

Various chemical, mechanochemical and mechanical activation methods of aluminum have been utilized so far [22, 30]. Many studies [1, 8, 19–23, 25–28, 30–40] demonstrated that an effective way of activating aluminum and achieving a high rate of hydrogen generation from its reaction with water is by alloying aluminum with metals

and nonmetals (Ga, Bi, Sn, In, Ca, Li, Zn, Mg, Ni, Co, Si, etc.). A number of papers showed that aluminum activated by alloying with low-melting metals is able to react with water already at room temperature [8, 22, 32, 33, 36, 37–40]. In the present study aluminum was activated by forming its alloys with an eutectic gallium-indium-tin alloy and with bismuth or antimony and the regularities of the hydrolysis of the obtained ESSs were studied.

The results of investigations of the thermophysical properties of an eutectic Ga–In–Sn alloy are given in [41, 42]. According to the data of different authors, Ga, In and Sn form an eutectic containing the following mass fractions of the components: 66.0...67.0% Ga, 20.5...22.0% In and 10.0...13.5% Sn. The melting point of these alloys is  $10.7 \pm 0.3^\circ\text{C}$  [42]. In [22] it is shown that the eutectic Ga–In–Sn alloy crystallizes during its cooling at a temperature  $28^\circ\text{C}$  lower than its melting point. Therefore, it can be assumed that aluminum activated in this alloy can interact with water at temperatures much lower than  $10.7 \pm 0.3^\circ\text{C}$ .

The structure of the alloys of aluminum with gallium, indium and tin, distribution of doping elements in alloys and regularities of their interaction with water were studied in a number of works [22, 32, 33, 36, 37]. An alloy containing 50 wt.% Al, 34 wt.% Ga, 11 wt.% In and 5 wt.% Sn was synthesized in [22]. It was found that at room temperature this alloy was partially liquid and reacted with distilled water generating hydrogen gas. Interaction between aluminum and water was facilitated due to the presence of a liquid alloy phase making a liquid window at the crystalline surface. The average yield of hydrogen was 83.8%. The aluminum oxidation product was bayerite, the other present alloy components did not react with water. Besides, an intermetallic compound  $\text{In}_3\text{Sn}$  was found in the hydrolysis products. As a result of the kinetics analysis performed in [22] it was found that the order of the reaction of aluminum with water was 0.7 and the activation energy was 43.8 kJ/mol.

The authors of [32] obtained alloys of aluminum with gallium (3.8 wt.%), indium (1.5 wt.%) and tin (0.7 wt.%). They were able to change the melt cooling rate and obtained the alloys with different crystallite sizes. Using EDS analysis they found the aluminum crystallites containing gallium with the atomic ratio  $\text{Al} : \text{Ga} \approx 60 : 1$  together with a small amount of indium and tin. The major amount of indium and tin was concentrated at the surface of crystallites. Using DSC the authors of [32] showed that the melting point of the grain boundary Ga–In–Sn phases was several degrees higher and the temperature of their crystallization was several tens of degrees lower than the melting point of the eutectic Ga–In–Sn alloy. The rate of interaction of such alloys with water increased with decreasing crystallite size and with increasing the temperature from 30 to  $60^\circ\text{C}$ . After immersion into water, solid samples of the alloys cracked within several seconds and formed powders. The reaction of the fine-grained samples with water proceeded rapidly and almost to a full completion, whereas the coarse-grained samples reacted with water with a slower rate and the hydrolysis was incomplete.

The kinetics of the interaction between the investigated alloys and water was determined using the following standard equation [32]:

$$\frac{d\alpha}{d\tau} = k(1 - \alpha)^n, \quad (4)$$

where  $\alpha$  is a degree of aluminum conversion;  $\tau$  is the reaction duration;  $k$  is a reaction rate constant;  $n$  is the reaction order for aluminum. The calculated values of the reaction order were between 0.64 and 0.72, and the activation energies decreased from  $77 \pm 8$  to  $53 \pm 4$  kJ/mol following a decrease in crystallite sizes from 258 to 23  $\mu\text{m}$ . According to [32], the liquid Ga–In–Sn alloy introduced into aluminum not only protected aluminum from oxidation, but also provided a path for the diffusion of its nanoparticles to the site of interaction with water. Furthermore, as aluminum reacted with water on

its bare surface, aluminum hydroxide, which was formed as a result of interaction between aluminum and water, could partially block the Al alloy surface and retard the process. However, because of vigorous hydrogen evolution no dense hydroxide layer was formed on the alloy surface. The authors of [32] explained the reaction order for aluminum of being less than one by the fact that aluminum interacted with water both on a bare crystalline surface, partially blocked by aluminum hydroxide, and on the spots covered with Ga–In–Sn alloy after diffusion through this alloy.

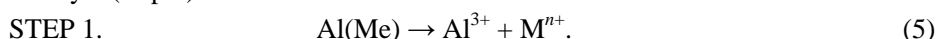
To study the effect of the microstructure and phase composition of Al–Ga–In–Sn alloy on the regularities of its interaction with water, the ribbons 40...60  $\mu\text{m}$  in thickness were made from the alloy ingots which were annealed in a temperature range of 250...500°C [36]. In the obtained ribbons a phase of solid solution of gallium in the aluminum and  $\text{In}_3\text{Sn}$  intermetallic phase were identified. Increasing the annealing temperature from 300 to 500°C led to an increase in the size of aluminum crystallites and Ga–In–Sn alloy particles on their surface, with the amount of ternary alloy particles decreasing. Studies of the interaction between the obtained activated aluminum ribbons and water at 30...60°C showed that the decrease in the aluminum crystallite size from 260 to 23  $\mu\text{m}$  led to an increase in hydrogen evolution rate, but when the crystallite size decreased further down to 3  $\mu\text{m}$ , the hydrogen evolution rate decreased to around 80% of its maximum value.

The effect of the composition of the Ga–In–Sn alloy on the aluminum activity in the reaction with water was studied in [37] by investigation of a series of aluminum-based alloys with constant total content of gallium, indium and tin (6 wt.%) but with variations in their ratio. These alloys interacted with water at the temperatures as low as 0.5°C; however, in the temperature range of 0.5...15°C their interaction rate was unstable. A stable increase in the rate of the aluminum hydrolysis was reached when the temperature raised above 15°C. At 50°C the solid samples of the alloys cracked after immersion into water and turned into powders within dozens of seconds. The hydrogen generation rate at 50°C vs gallium content had a maximum at the gallium content of 3.8 wt.%. Using XRD study it was concluded that at the indium-to-tin ratio of 15 : 7 the studied alloys contained a solid solution of gallium in aluminum and  $\text{In}_3\text{Sn}$  intermetallic phase [37]. When the tin content increased to the ratio  $\text{In} : \text{Sn} = 1 : 1$ , an  $\text{InSn}_4$  intermetallic phase was also identified. Such increase of the tin content in the investigated alloys led to a significant (~50%) increase in hydrogen generation rate, which was explained by the formation of the aluminum-tin microgalvanic couples. In such a case the aluminum was dissolved anodically, and cathodic hydrogen evolution from water took place on the tin-rich particles.

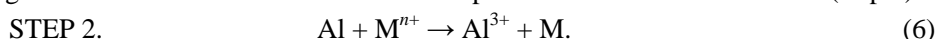
The Al–Ga–Sn (1.73 wt.% Ga, 1 wt.% Sn) and Al–Ga–In (1.73 wt.% Ga, 1 wt.% In) alloys were obtained and investigated in [33]. At 30°C the highest hydrogen evolution rate was achieved during the hydrolysis of the Al–Ga–Sn alloy and the lowest rate was observed during the hydrolysis of the Al–Ga–In alloy. It was concluded that the rate of the interaction between the alloys and water was determined by the difference in electrode potentials between aluminum and added metals. Based on the theory of microgalvanic couples, the potential differences in the Al–Sn, Al–In and Al–Ga couples were calculated. These differences were the largest for the Al–Sn couple (–1.53 V) and the smallest for the Al–Ga couple (–1.15 V), i.e. the potential differences decreased in the order  $\text{Al–Sn} > \text{Al–In} > \text{Al–Ga}$ , which corresponded to the sequence of decrease in the aluminum dissolution rate during interaction of the studied alloys with water [33].

The activation effect of the more electropositive than aluminum metals introduced into aluminum on its corrosive dissolution were considered in a number of reference works [34, 43–45]. As a result of the formation of microgalvanic couples, the potential of aluminum shifted to the negative values, which caused its rapid dissolution. The three-step mechanism of activation of the aluminum anodes, proposed in [43], envisages

the dissolution of aluminum occurring after the immersion of the alloy in a solution of an electrolyte (step 1):



Then the cations of more electropositive metal are reduced as a result of electron exchange with aluminum and the metal forms deposits on the aluminum surface (step 2):



Step 3 occurs simultaneously with step 2 and consists of a local detachment of the protective oxide film formed on the aluminum surface, which is caused by the presence of a more electropositive metal on its surface:

STEP 3. Local detachment of the protective oxide film.

As a result the aluminum surface becomes locally free of the protective film and the aluminum potential shifts to the more negative values. Similar mechanisms are also proposed in [8, 34].

As both aluminum and gallium belong to the IIIA subgroup of the periodic table they can readily form a solid solution [8]. Gallium and aluminum have close values of atomic radii (1.41 Å and 1.43 Å, respectively); therefore, gallium can be dissolved in aluminum without significant aluminum lattice distortion. Indeed, according to the phase diagram of the Al–Ga system the solubility of Ga in Al is 20 wt.% [34].

Indium is slightly soluble in aluminum. According to the phase diagram of the Al–In system, its solubility in Al is 0.01...0.05 wt.% [34]. The introduction of indium into aluminum in amounts exceeding its solubility limit results in the crystallization of indium on the surface of aluminum crystallites as an individual phase. Tin has also a low solubility in aluminum and forms in the presence of indium in the alloy the intermetallic compounds with In, which are formed on the aluminum surface. The composition of In–Sn intermetallics depends on the ratio In : Sn in the alloy. As an example in the alloy containing 97 wt.% Al, 1.75 wt.% Ga, indium and tin the only formed at a tin content of < 0.35 wt.% intermetallic is  $\beta\text{-In}_3\text{Sn}$  [35]. Increase in the tin content from 0.35 to 0.9 wt.% leads to an increase in the  $\gamma\text{-InSn}_4$  content and a decrease in the  $\beta\text{-In}_3\text{Sn}$  content. At the tin content of > 0.9 wt.%, only the  $\gamma\text{-InSn}_4$  phase was observed. The particles of In–Sn intermetallics formed on the surface of the aluminum crystallites create the microgalvanic couples with aluminum which facilitates aluminum dissolution. The authors of [35] also found that the rate of  $\text{H}_2$  generation by the interaction of Al–Ga–In–Sn alloy with water vs the content of tin in the temperature range of 60...75°C has a maximum at the tin content of 0.5 wt.%, which corresponds to the maximum amount of the  $\beta\text{-In}_3\text{Sn}$  phase present at the surface of Al crystallites.

Thus, the temperature at which the aluminum-based ESSs react with water, reaction rate and hydrogen yield depend on the nature of added metals-activators, their content in ESS and alloy preparation conditions. It should be also noted that the storage duration and conditions of the ESSs based on aluminum activated with liquid metals and alloys are important for the extent of their activity and hydrogen yield during their interaction with water. According to the results obtained in [31], the alloy of aluminum (80 wt.%) with gallium, indium, tin and zinc retained its activity only after storage at liquid nitrogen temperature. The storage of alloys in vacuum, in an inert atmosphere and particularly in air leads to a decrease in hydrogen yield during the interaction between alloys and water. However, in [37] it is shown that bulk samples of activated aluminum retain their activity during at least one month when stored in dry air with humidity below 20%. Therefore, for the long-term storage of the aluminum-based ESSs it is important to seal them in plastic bags filled with an inert gas.

The eutectic Ga–In–Sn alloy introduced into aluminum essentially acts as a catalyst in the reaction of aluminum with water since the alloy components accelerate the disso-

lution of aluminum but do not react with water [22]. The amount of the eutectic Ga–In–Sn alloy which is used to activate aluminum must be above a minimum value for achieving the required hydrogen generation rate at a given temperature. It is shown that aluminum activated with the eutectics Ga–In–Sn generates hydrogen from water at 25°C if the content of this alloy is  $\geq 3$  wt.% [46]. However, the activity of such aluminum-based ESSs can decrease with time. That is why, in this study the amount of eutectic Ga–In–Sn alloy introduced into aluminum was 5 wt.%. Furthermore, to study the effect of electropositive additives on the regularities of interaction between activated aluminum and water, additions of bismuth or antimony (3 wt.% each) were introduced into the studied alloys.

**Experimental.** To prepare the aluminum-based ESSs, high-purity metals ( $\geq 99.9$  wt.%) were used. The eutectic Ga–In–Sn alloy with mass fractions of the components of 67/22/11% was prepared by adding required weighted amounts of indium powder and tin to a molten gallium kept at 50°C. The mixture was held at 50°C for 30 min with periodic stirring. After cooling down to room temperature the obtained alloy remained liquid.

Aluminum with appropriate additions of eutectic Ga–In–Sn alloy and Bi or Sb was melted in an electric shaft furnace in an argon atmosphere with mechanical stirring. A calculated amount of aluminum was placed in an alundum crucible inserted into electric furnace. The crucible was covered with a quartz cover with holes for feeding argon and placing an alundum stirrer. Argon was introduced into the crucible using a quartz tube. The aluminum was melted at 900°C, and calculated amounts of the pre-prepared eutectic Ga–In–Sn alloy and Bi or Sb were added to the molten metal. After that, the melt was stirred for 30 min with an alundum blade stirrer connected to an electric motor. The melt was quickly poured into a flat rectangular graphite mold. The thickness of the melted layer in the mold was below 5 mm, which ensured a high rate of its cooling. After cooling the obtained alloys were sealed in the double polyethylene bags filled with a high-purity argon.

The regularities of hydrogen evolution during interaction between the obtained ESSs and water were studied by measuring the volume of evolved hydrogen. A setup for volumetric measurements consisted of a thermostated beaker, a connecting tube and an eudiometer. 100 ml of distilled water was poured into the baker which was presaturated with hydrogen. After that the alloy sample of 1 g in the form of a rectangular parallelepiped was placed into water. The beaker was hermetically sealed. Hydrogen that evolved during aluminum hydrolysis entered the eudiometer where its volume was measured at regular intervals. The water temperature was kept constant by using a U-4 thermostat.

The average rate of hydrogen evolution within the time of interaction between alloys and water was determined from

$$v = \frac{V_0}{\tau}, \quad (7)$$

where  $V_0$  is the volume of  $H_2$  (at normal conditions) which evolved within time  $\tau$ .

The evolved hydrogen volume was converted to normal conditions (T 273.15 K, pressure 760 mm Hg) according to the formula:

$$V_0 = \frac{273.15 \cdot V_\tau \cdot (P - p - \frac{h_{H_2O}}{13.6})}{760(273.15 + t)}, \quad (8)$$

where  $V_\tau$  is a volume of hydrogen measured at room temperature  $t$  (°C) and the barometric pressure  $P$  (mm·Hg);  $p$  is a water vapor pressure (mm·Hg) at the same temperature;  $h_{H_2O}$  is a water column height in the eudiometer (mm); 13.6 is the mercury density (g/cm<sup>3</sup>).

**Results and discussion.** Bismuth and antimony which have positive values of standard electrode potentials ( $E_{\text{Bi}^{3+}/\text{Bi}}^{\circ} = 0.20 \text{ V}$ ,  $E_{\text{Sb}^{3+}/\text{Sb}}^{\circ} = 0.24 \text{ V}$  [29]) were chosen as additives to the aluminum activated with the Ga–In–Sn eutectic alloy. The standard electrode potential difference between aluminum and bismuth is  $-1.862 \text{ V}$  and between aluminum and antimony is  $-1.902 \text{ V}$ . The obtained and investigated aluminum-based alloys contain 5 wt.% eutectic Ga–In–Sn alloy and 3.0 wt.% Bi or Sb.

As can be seen from Fig. 1 the introduction of bismuth into aluminum activated by Ga–In–Sn eutectic led to a significant decrease in  $\text{H}_2$  generation rate. However, the introduction of antimony into activated aluminum changed only slightly the regulations of hydrogen evolution: they were close to those of hydrogen evolution during the hydrolysis of aluminum activated with the Ga–In–Sn eutectic only.

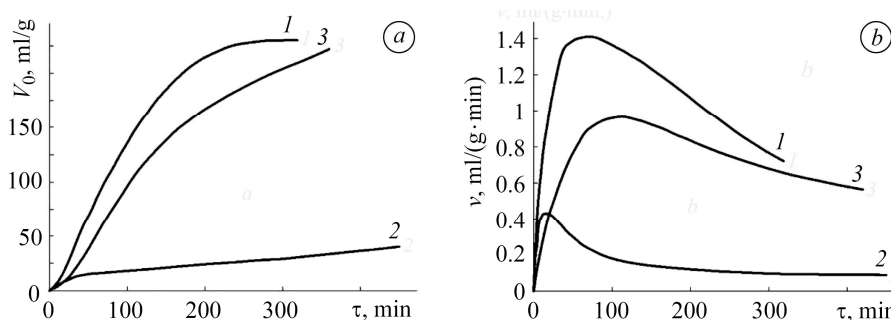


Fig. 1. Time dependences of the volume of generated hydrogen (a) and average rate of its evolution (b) during hydrolysis of aluminum activated by the eutectic Ga–In–Sn alloy (5 wt.%) (1) and bismuth (3 wt.%) (2) or antimony (3 wt.%) (3) measured at 25°C.

At the beginning of interaction between the investigated ESSs and water, a sharp increase in hydrogen evolution rate occurred as a result of the activation and growth of the reacting aluminum surface, particularly when the samples were cracked and disintegrated. However, after the consumption of the main amount of aluminum, the hydrogen accumulation rate decreased, thus, the plots of  $v$  vs  $\tau$  contained maxima. The samples of the activated aluminum with an additive of bismuth did not crack during hydrolysis. Therefore, after the completion of the period of activation of their surface, the  $v - \tau$  plots showed only a mostly constant rate of hydrogen generation, which is important for the simplification of the hydrogen supply system of fuel cells. Thus, the effect of bismuth and antimony on the activity of aluminum differed greatly, though bismuth and antimony have close values of standard electrode potential. The electrochemical properties of these additives do not apparently determine their effect on the regularities of interaction between Al and water. However, the alloy formation process changed by additives and their ability to form the intermetallics with other components of the investigated ESSs are of crucial importance, which calls for the additional studies.

Raising the hydrolysis temperature of all alloys from 25 to 70°C led to a significant increase in the volume of evolved hydrogen and a decrease in the duration of their hydrolysis (see Fig. 2). It should be noted that the sigmoidal shape of the obtained  $V_0 - \tau$  plots containing a bend is typical of the topochemical reactions, i.e. heterochemical reactions, which proceed for the solids [47, 48].

Hydrogen yield sharply increased with increasing temperature, and the time to reach its maximum values was significantly reduced. As example, for Al–Ga–In–Sn alloy hydrolysis at the temperature of 25°C for 320 min only 19.5% of the hydrogen from the theoretically possible amount was evolved, whereas at 70°C the hydrogen yield was 98.8% after 23 min. Al–Ga–In–Sn–Bi alloy was less active and the hydrogen yield at 25°C during its hydrolysis for 450 min was only 3.5%; however, the hydrolysis at 70°C

for 120 min resulted in hydrogen yield of 99.3%. When using Al–Ga–In–Sn–Sb alloy, hydrogen yield during hydrolysis at 25°C for 420 min amounted to 20.7%, but at 70°C after 70 min it increased to 99.7%.

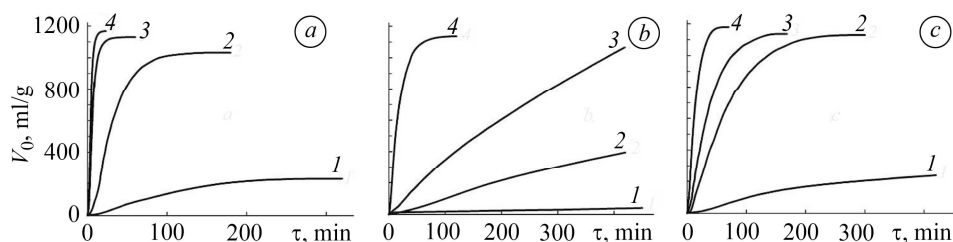


Fig. 2. Time dependences of hydrogen volume evolved during the hydrolysis of aluminum activated with the eutectic Ga–In–Sn alloy (a) and bismuth (b) or antimony (c) at the temperatures (°C): 25 (1); 40 (2); 55 (3); 70 (4).

Most  $v - \tau$  plots have maxima, which are reached faster and are higher with increasing the hydrolysis temperature (see Fig. 3). Raising the temperature from 25 to 70°C led to a significant increase in the maximum rate of hydrogen generation during the hydrolysis of all investigated alloys. In particular, during the hydrolysis of aluminum activated with the Ga–In–Sn eutectic only, the maximum value of  $v$  increased by 2 orders of magnitude (from 1.42 to 158.6 mL/(g·min)). Large plateau can be seen in the  $v - \tau$  plots during the hydrolysis of activated aluminum with additive of bismuth at 25...55°C when hydrogen was generated at almost constant rate.

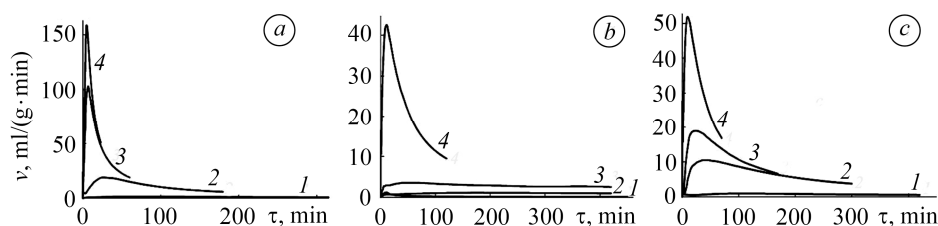


Fig. 3. Average rates of hydrogen evolution during the hydrolysis of aluminum activated with the eutectic Ga–In–Sn alloy (a) and bismuth (b) or antimony (c) versus the time of hydrolysis at the temperature (°C): 25 (1); 40 (2); 55 (3); 70 (4).

To determine the effective rate constants ( $k^e$ ) of aluminum hydrolysis reactions during interaction between the aluminum-based ESSs and water, the Prout–Tompkins equation was utilized which describes the topochemical reactions of decomposition of solid materials through the crystalline cracking proceeding at the boundary between them and the solid decomposition product [47–49]:

$$\ln[1/(1 - \alpha)] = k^e \tau + C, \quad (9)$$

where  $C$  is an integration constant. In the differential form, Eq. (9) looks like:

$$d\alpha/d\tau = k^e \alpha(1 - \alpha), \quad (10)$$

from which it follows that the reaction rate depends both on the amount of reacting substance and on the amount of product. Such reactions belong to the autocatalytic processes [49].

The degree of aluminum conversion was calculated as the ratio between the hydrogen volume evolved and the theoretical value which would form as a result if the hydrolysis reaction would be complete. The clearly developed linear sections were not present in the plots of  $\ln[\alpha/(1 - \alpha)]$  vs  $\tau$ . Because of that, the modified Prout–



Tompkins equation presenting an inverse variation of the effective rate constant of the topochemical reaction on time,

$$\ln[\alpha/(1 - \alpha)] = k^e \ln \tau + C \quad (11)$$

should be applied [49]. All obtained plots  $\ln[\alpha/(1 - \alpha)] - \ln \tau$  (see Fig 4) contained an induction period of interaction which was common for the topochemical reactions [47, 48]. After the induction period was finished, the dependences showed the presence of the prolonged linear sections. Finally, when linear intervals were over, the curves showed start of the retardation process.

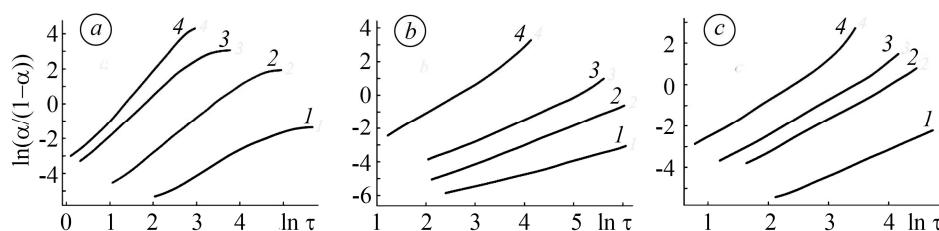


Fig. 4. Plots of  $\ln[\alpha/(1 - \alpha)]$  vs  $\ln \tau$  obtained during the hydrolysis of aluminum activated with the eutectic Ga–In–Sn alloy (a) and bismuth (b) or antimony (c) at the temperatures (°C): 25 (1); 40 (2); 55 (3); 70 (4).

The values of the effective rate constants of the interaction between aluminum and water were determined as the slope of the linear sections of the plots shown in Fig. 4 (see Table). The highest values of  $k^e$  were observed during the hydrolysis of activated aluminum without Bi or Sb additives. Rising the temperature from 25 to 70°C led to an increase in the values of  $k^e$  for all studied ESSs.

**Effective rate constants and activation energies for the hydrolysis of aluminum activated with the eutectic Ga–In–Sn alloy and Bi or Sb at various temperatures**

Alloy	Temperature (°C)				$E_a$ , kJ/mol
	25	40	55	70	
	$k^e$ , min <sup>-1</sup>				
Al + 5 wt.% Ga–In–Sn	1.46	1.98	2.33	2.90	12.60
Al + 5 wt.% Ga–In–Sn + 3 wt.% Bi	0.81	1.17	1.34	1.73	13.75
Al + 5 wt.% Ga–In–Sn + 3 wt.% Sb	1.27	1.58	1.69	1.88	7.10

The temperature dependences of the effective rate constants of the hydrolysis of the investigated ESSs were used to calculate the activation energies of this process according to the Arrhenius equation (see Table). The obtained activation energy values are low and indicate that the hydrolysis of the investigated aluminum-based ESSs proceeds as a diffusion-controlled process starting after the end of the induction period and finishing before the process deceleration develops.

**CONCLUSIONS**

Aluminum activation by addition of the eutectic Ga–In–Sn alloy, bismuth or antimony dramatically improves the performance of individual Al metal used in hydrolysis process to generate hydrogen gas by interaction with water at the temperatures exceeding 25°C. The most efficient performance in the hydrolysis reaction has been achieved for aluminum doped with Ga–In–Sn eutectic (5 wt.%) only. Bulk samples of this alloy crack and become decrepitated when interacting with water during the progression of the hydrolysis process. It appears that the additives of bismuth and antimony differently affect the regularities of the hydrolysis of activated aluminum

despite of the close values of their standard electrode potentials. Indeed, while additions of bismuth (3 wt.%) into the Al–Ga–In–Sn alloy significantly reduce the hydrolysis rate, additions of antimony (3 wt.%) lead to a slight decrease in the hydrolysis rate only. However, in the temperature range 25...55°C, an almost constant rate of hydrogen generation can be achieved for a long period of time for the Al–Ga–In–Sn alloy doped with 3 wt.% of Bi. Such slower interaction is not accompanied by cracking and powdering of the bulk alloy samples.

The kinetics of the hydrogen generation process is described by sigmoid-shaped plots of the time dependence of the generated hydrogen volume indicating that the reactions of the investigated alloys with water are topochemical processes. The values of the effective rate constants of the hydrolysis for all studied alloys are determined using the modified Prout–Tompkins equation and show an increase when the temperature is rising from 25 to 70°C. The values of activation energy of hydrolysis process, calculated from the temperature dependence of the effective rate constants indicate that the hydrolysis is a diffusion-controlled process which further to the intensive H<sub>2</sub> generation part contains the induction period and the retardation step of the interaction of the alloy with water.

*РЕЗЮМЕ.* Досліджено каталізовану евтектикою Ga–In–Sn взаємодію алюмінієвих сплавів з водою, в результаті якої відбувається гідроліз алюмінію та генерується водень. Приготовано сплави алюмінію з евтектикою Ga–In–Sn (5 wt.%), а також з вісмутом (3 wt.%) або сурмою (3 wt.%) і за результатами волюмометричних вимірювань водню вивчено кінетику їх гідролізу в температурному діапазоні 25...70°C. Найефективніше гідроліз алюмінію активується використанням сплаву Al–Ga–In–Sn. Введення вісмуту у сплав Al–Ga–In–Sn значно знижує швидкість гідролізу алюмінію, тоді як введення сурми несуттєво впливає на протікання процесу, хоча стандартні електродні потенціали вісмуту і сурми мають близькі значення. Реакції досліджених сплавів з водою добре описуються як топохімічні процеси. Зі застосуванням модифікованого рівняння Прута–Томпкінса розраховано ефективні константи швидкості гідролізу усіх сплавів і встановлено, що вони збільшуються зі зростанням температури від 25 до 70°C. За температурною залежністю ефективних констант швидкості розраховано енергії активації гідролізу досліджених сплавів, які свідчать, що впродовж основного періоду генерації водню (після завершення індукційного періоду і до початку сповільнення виділення водню) процес протікає з дифузійними обмеженнями швидкості.

**Ключові слова:** *гідроліз, сплави алюмінію, одержання водню, евтектичний сплав Ga–In–Sn, кінетика гідролізу.*

*РЕЗЮМЕ.* Исследовано катализируемое эвтектикой Ga–In–Sn взаимодействие алюминиевых сплавов с водой, в результате которого происходит гидролиз алюминия и генерируется водород. Приготовлено сплавы алюминия с эвтектикой Ga–In–Sn (5 wt.%), а также с висмутом (3 wt.%) или сурьмой (3 wt.%), и по результатам волюмометрических измерений водорода изучено кинетику их гидролиза в температурном диапазоне 25... 70°C. Наиболее эффективно гидролиз алюминия активируется использованием сплава Al–Ga–In–Sn. Введение висмута в сплав Al–Ga–In–Sn значительно снижает скорость гидролиза алюминия, тогда как введение сурьмы несущественно влияет на протекание процесса, хотя стандартные электродные потенциалы висмута и сурьмы имеют близкие значения. Реакции исследованных сплавов с водой хорошо описываются как топохимические процессы. С применением модифицированного уравнения Прута–Томпкинса рассчитано эффективные константы скорости гидролиза всех сплавов и установлено, что они возрастают с повышением температуры от 25 до 70°C. По температурной зависимости эффективных констант скорости рассчитано энергии активации гидролиза исследованных сплавов, которые свидетельствуют, что на протяжении основного периода генерации водорода (после завершения индукционного периода и до начала замедления выделения водорода) процесс протекает с диффузионными ограничениями скорости.

**Ключевые слова:** *гидролиз, сплавы алюминия, получение водорода, эвтектический сплав Ga–In–Sn, кинетика гидролиза.*

**Acknowledgements.** *This work received a support from NATO SPS program (Project G5233 Portable Energy Supply). The authors are grateful to Prof. I. Yu. Zavalij for his help.*

1. Козин Л. Ф., Волков С. В. Современная энергетика и экология: проблемы и перспективы. – К.: Наук. думка, 2006. – 775 с.
2. Ramachandran R. and Menon R. K. An overview of industrial uses of hydrogen // Int. J. Hydrogen Energy. – 1998. – **23**, № 7. – P. 593–598.
3. Winter C.-J. Hydrogen energy – Abundant, efficient, clean: A debate over the energy-system-of-change // Int. J. Hydrogen Energy. – 1998. – **34**, № 14. – P. S1–S52.
4. Тарасов Б. П., Лотоцкий М. В. Водородная энергетика: прошлое, настоящее, виды на будущее // Рос. хим. журн. – 2006. – **50**, № 6. – С. 5–18.
5. Goltsov V. A., Veziroglu T. N., and Goltsova L. F. Hydrogen civilization of the future – A new conception of the IAHE // Int. J. Hydrogen Energy. – 2006. – **31**, № 2. – P. 153–159.
6. Gröger O., Gasteiger H. A., and Suchsland J. -P. Review – Electromobility: Batteries or Fuel Cells? // J. Electrochem. Soc. – 2015. – **162**, № 14. – P. A2605–A2622.
7. Fuel Cell Fundamentals, 3rd Edition / R. O'Hayre, Cha Suk-Won, W. Colella, and F. B. Prinz. – Hoboken, NJ: John Wiley & Sons, Inc., 2016. – 600 p.
8. Hu S., Zhao X., and Liu J. Liquid metal activated aluminum-water reaction for direct hydrogen generation at room temperature // Renew. Sustain. Energy Reviews. – 2018. – **92**. – P. 17–37.
9. Fuel Cells and Hydrogen Production / Eds.: T. E. Lipman, A. Z. Weber. – NY: Springer, 2019. – 1179 p.
10. Hydrogen generation from water electrolysis – possibilities of energy saving / D. Lj. Stojić, M. P. Marčeta, S. P. Sovilj, Šć. S. Miljanić // J. Power Sources. – 2003. – **118**, № 1–2. – P. 315–319.
11. Integrated hydrogen production options based on renewable and nuclear energy sources / M. F. Orhan, I. Dincer, M. A. Rosen, and M. Kanoglu // Renew. Sustain. Energy Reviews. – 2012. – **16**, № 8. – P. 6059–6082.
12. Yildiz B. and Kazimi M. S. Efficiency of hydrogen production systems using alternative nuclear energy technologies // Int. J. Hydrogen Energy. – 2006. – **31**, № 1. – P. 77–92.
13. Kandi D., Martha S., and Parida K. M. Quantum dots as enhancer in photocatalytic hydrogen evolution: A review // Int. J. Hydrogen Energy. – 2017. – **42**, № 15. – P. 9467–9481.
14. Sharma P. and Kolhe M. L. Review of sustainable solar hydrogen production using photon fuel on artificial leaf // Int. J. Hydrogen Energy. – 2017. – **42**, № 36. – P. 22704–22712.
15. Yilmaz F., Balta M. T., and Selbaş R. A review of solar based hydrogen production methods // Renew. Sustain. Energy Reviews. – 2016. – **56**. – P. 171–178.
16. Hydrogen from photo-catalytic water splitting process: A review / H. Ahmad, S. K., Kamarudin L. J. Minggu, and M. Kassim // Renew. Sustain. Energy Reviews. – 2015. – **43**. – P. 599–610.
17. Tanksale A., Beltramini J. N., and Lu G. M. A review of catalytic hydrogen production processes from biomass // Renew. Sustain. Energy Reviews. – 2010. – **14**, № 1. – P. 166–182.
18. Effective hydrogen production using waste sludge and its filtrate / L. Guo, X. M. Li, G. M. Zeng, and Y. Zhou // Energy. – 2010. – **35**, № 9. – P. 3557–3562.
19. Варшавский И. Л. Энергоаккумулирующие вещества и их использование. – К.: Наук. думка, 1980. – 240 с.
20. Водород-генерирующие материалы для источников водорода гидролизного типа / Р. С. Назаров, С. Д. Куш, О. В. Кравченко, Э. Э. Фокина, Б. П. Тарасов // Альтернативная энергетика и экология. – 2010. – № 6(86). – С. 26–32.
21. Aluminum and aluminum alloys as sources of hydrogen for fuel cell applications / L. Soler, J. Macanás, M. Muñoz, and J. Casado // J. Power Sources. – 2007. – **169**, № 1. – P. 144–149.
22. Liquid phase-enabled reaction of Al–Ga and Al–Ga–In–Sn alloys with water / J. T. Ziebarth, J. M. Woodall, R. A. Kramer, and G. Choi // Int. J. Hydrogen Energy. – 2011. – **36**, № 9. – P. 5271–5279.
23. Parmuzina A. V. and Kravchenko O. V. Activation of aluminum metal to evolve hydrogen from water // Int. J. Hydrogen Energy. – 2008. – **33**, № 12. – P. 3073–3076.
24. Hydrogen generation by oxidation of coarse aluminum in low content alkali aqueous solution under intensive mixing / G. N. Ambaryan, M. S. Vlaskin, A. O. Dudoladov, E. A. Meshkov, A. Z. Zhuk, and E. I. Shkolnikov // Int. J. Hydrogen Energy. – 2016. – **41**, № 39. – P. 17216–17224.
25. Rosenband V. and Gany A. Application of activated aluminum powder for generation of hydrogen from water // Int. J. Hydrogen Energy. – 2010. – **35**, № 20. – P. 10898–10904.

26. *Ilyukhina A. V., Ilyukhin A. S., and Shkolnikov E. I.* Hydrogen generation from water by means of activated aluminum // *Int. J. Hydrogen Energy.* – 2012. – **37**, № 21. – P. 16382–16387.
27. *Babak A. and Korosh M.* A novel method for generating hydrogen by hydrolysis of highly activated aluminum nanoparticles in pure water // *Int. J. Hydrogen Energy.* – 2009. – **34**, № 19. – P. 7934–7938.
28. *Korosh M. and Babak A.* Enhancement of hydrogen generation in reaction of aluminum with water // *Int. J. Hydrogen Energy.* – 2010. – **35**, № 11. – P. 5227–5232.
29. *Milazzo G. and Caroli S.* Tables of Standard Electrode Potentials. – NY: Wiley, 1978. – 421 p.
30. *Shkolnikov E. I., Zhuk A. Z., and Vlaskin M. S.* Aluminum as energy carrier: Feasibility analysis and current technologies overview // *Renewable and Sustainable Energy Reviews.* – 2011. – **15**, № 9. – P. 4611–4623.
31. *Activation of aluminum metal and its reaction with water / O. V. Kravchenko, K. N. Semenenko, B. M. Bulychev, and K. B. Kalmykov // J. Alloys & Compounds.* – 2005. – **397**, № 1–2. – P. 5227–5232.
32. *Wang W., Chen D. M., and Yang K.* Investigation on microstructure and hydrogen generation performance of Al-rich alloys // *Int. J. Hydrogen Energy.* – 2010. – **35**, № 21. – P. 12011–12019.
33. *Reactivity of Al-rich Alloys with Water Promoted by Liquid Al Grain Boundary Phases / T. He, W. Wang, W. Chen, W. Chen, D. Chen, and K. Yang // J. Mat. Sci. & Techn.* – 2017. – **33**, № 4. – P. 397–403.
34. *effects of preparation parameters and alloy elements on the hydrogen generation performance of aluminum alloy – 0°C pure water reaction / C. Ying, L. Bei, W. Huihu, and D. Shijie // Rare Metal Materials and Eng.* – 2017. – **46**, № 9. – P. 2428–2432.
35. *Influence of In and Sn compositions on the reactivity of Al–Ga–In–Sn alloys with water / T. T. He, W. Wang, W. Chen, D. M. Chen, and K. Yang // Int. J. Hydrogen Energy.* – 2017. – **42**, № 9. – P. 5627–5637.
36. *Insight into the reactivity of Al–Ga–In–Sn alloy with water / W. Wang, X. M. Zhao, D. M. Chen, and K. Yang // Int. J. Hydrogen Energy.* – 2012. – **37**, № 3. – P. 2187–2194.
37. *Effect of composition on the reactivity of Al-rich alloys with water / W. Wang, W. Chen, X. M. Zhao, D. M. Chen, and K. Yang // Int. J. Hydrogen Energy.* – 2012. – **37**, № 24. – P. 18672–18678.
38. *Wang C. C., Chou Y. C., and Yen C. Y.* Hydrogen generation from aluminum and aluminum alloys powder // *Proc. Eng.* – 2012. – **36**. – P. 105–113.
39. *A review on hydrogen production using aluminum and aluminum alloys / H. Z. Wang, D. Y. C. Leung, M. K. H. Leung, and M. Ni // Renewable and Sustainable Energy Reviews.* – 2009. – **13**, № 4. – P. 845–853.
40. *Fan M. Q., Xu F., and Sun L. X.* Studies on hydrogen generation characteristics of hydrolysis of the ball milling Al-based materials in pure water // *Int. J. Hydrogen Energy.* – 2007. – **32**, № 14. – P. 2809–2815.
41. *Evans D. S. and Prince A.* Thermal analysis of Ga–In–Sn system // *Metal Sci.* – 1978. – **12**, № 9. – P. 411–414.
42. *Thermophysical properties of the liquid Ga–In–Sn eutectic alloy / Yu. Plevachuk, V. Sklyarchuk, Sv. Eckert, G. Gerbeth, and R. Novakovic // J. Chem. Eng. Data.* – 2014. – **59**, № 3. – P. 757–763.
43. *Reboul M. C., Gimenez Ph., and Rameau J. J.* A Proposed activation mechanism for Al anodes // *Corrosion.* – 1984. – **40**, № 7. – P. 366–371.
44. *Breslin C. B. and Carroll W. M.* The electrochemical behavior of aluminum activated by gallium in aqueous electrolytes // *Corr. Sci.* – 1992. – **33**, № 11. – P. 1735–1746.
45. *Venugopal A. and Raja V. S.* AC impedance study on the activation mechanism of aluminum by indium and zinc in 3.5% NaCl medium // *Corr. Sci.* – 1997. – **39**, № 12. – P. 2053–2065.
46. *Закономірності гідролізу алюмінію, активованого евтектичним сплавом галію, індію та олова / Ф. Д. Манілевич, Л. Х. Козін, Б. І. Данильцев, А. В. Куций, Ю. К. Пірський // Укр. хім. журн.* – 2017. – **83**, № 7. – С. 51–59.
47. *Дельмон Б.* Кинетика гетерогенных реакций. – М.: Мир, 1972. – 556 с.
48. *Барре П.* Кинетика гетерогенных процессов. – М.: Мир, 1976. – 400 с.
49. *Brown M. E.* The Prout–Tompkins rate equation in solid-state kinetics // *Thermochim. Acta.* – 1997. – **300**, № 1–2. – P. 93–106.

Received 12.04.2019